2008 IEEE International Conference on
Robotics and Automation
Pasadena, CA, USA, May 19-23, 2008

Fabrication of biodegradable scaffolds by use of self-assembled magnetic sugar particles as a casting template

Tomoyuki Uchida[1], Hiroyuki Oura[1], Seiichi Ikeda[1], Fumihito Arai[2], Makoto Negoro[3], Toshio Fukuda[1]

Abstract— **Technologies to develop scaffolds with controlled pore layout and porosity have great significance in tissue engineering. As one method of scaffold fabrication, porogen leaching has been commonly used to control pore size, pore structure and porosity in the scaffold. In this paper, we describe a novel approach to fabricate 2D and 3D porous biodegradable scaffolds made of poly(L-lactide-co-ε-caprolactone) by using magnetic sugar particles as porogens. First, ferrite micro/nano particles were encapsulated in sugar microspheres to make them magnetized. After sieving magnetic sugar particles, those diameter-controlled particles were attracted by a magnetic force to form an assembled template for polymer casting. A magnetic field with polka-dot pattern was also utilized to align particles on desired positions. After polymer casting and removal of the sugar template, spherical pores were generated inside scaffold. For future application in vascular tissue engineering, we extended the scaffold fabrication to straight tubular scaffolds by winding 2D porous sheets on sacrificial molds. The biocompatibility of the developed scaffold was confirmed by viable cells after 4-day culture.**

I. Introduction

Recent progress in regenerative medicine is receiving attentions as a representative treatment for organ transplantation. One main approach to regenerate tissues is to reproduce an artificial organ in-vitro first and then transfer it into a patient's body[1,2]. For in-vitro preparation of tissues, tissue engineering is very important in terms of developing scaffolds that restore, maintain, and improve functions of damaged tissue[3]. The development of appropriate 3D scaffolds for the maintenance of cellular viability is important and has been a challenge in the field of tissue engineering. Additionally, the development of biomimetic vascular constructs is also very useful to evaluate robotic manipulation of catheters for the training of endovascular surgery. While scaffold materials must hold biocompatibility and appropriate degradation speed for implantation, an ideal scaffold should have 3D well-connected macro and micro porous structure to accommodate cells and to facilitate the transportation of nutrient. In previous studies, microscopic and macroscopic 3D porous structure has been fabricated by various methods such as porogen leaching[4], electrospinning[5], multilayer lamination[6], molding[7], 3D printing[8] and phase separation[9]. Above all methods, porogen leaching has an absolute advantage that the size of porogens can be controlled easily by using sieves, thereby ensuring pores with controlled size.

Two main techniques have been used to achieve well-connected pores and high porosity inside the scaffolds by porogen leaching. Murphy et al. proposed a way to improve pore connectivity by salt fusion under moderate humidity and temperature[10]. On the other hand, Wei et al. proposed another unique way to enhance the pore connectivity by emulsified sugar spheres[11]. Well-connected pores with uniform diameter should be very useful for effective and fast regeneration of tissue. In addition to all of these previous efforts, manipulation and assembly of porogens are also interesting and has great potential to achieve patterned and well-connected pores in a scaffold. Magnetically-guided self-assembly has been used to form fibrin matrices[12] and cellular constructs for tissue engineering[13]. However, it was never used to control the pore layout inside scaffolds[14]. Here, we propose a novel way to fabricate flat and tubular constructs with patterned pores by use of magnetic sugar particles. The developed scaffolds had ordered and well-connected micropores. The safeness of fabrication process was confirmed by the viability of human umbilical vein endothelial cells (HUVECs).

II. Materials and Methods

2.1 Materials and equipments

Poly(L-lactide-co-ε-caprolactone, PLCL) (C_{LA} : C_{CL} = 52:48, M_w = 540,000) as biodegradable polymer was purchased from BMG (Japan). D-fructose (m.p. 102-104 °C), sorbitanmonooleate (Span 80, surfactant) were purchased from Sigma (St. Louis, MO). Mineral oil and hexane were from Wako Pure Chemical (Japan). Ferrite particles (average size: 1 μm) were kindly donated from Toda Kogyo (Japan). Disk-type neodymium magnets (Magnetic flux density: 0.12 and 0.38 T) were purchased from Seiko Sangyo (Japan). HUVECs and HuMedia EG2 were purchased from Kurabo (Japan). D-PBS, carbonic acid buffer, HEPES were purchased from Wako Pure Chemical. 0.5% type I collagen solution and SYTO 13 were purchased from Koken (Japan) and Invitrogen (USA), respectively.

An inverted optical microscope (IX-71, Olympus Co.Ltd., Japan) was used to observe MSPs and viable HUVECs. A stereomicroscope (VHX-900, KEYENCE Co.Ltd., Japan)

1 Dept. of Micro- Nano Systems Engineering, Graduate School of Engineering, Nagoya University, Furo-cho 1, Chikusa-ku, Nagoya city, Aichi, 464-8603 JAPAN

2 Dept. of Bioengineering and Robotics, Graduate School of Engineering, Tohoku University, 6-6-01 Aramaki-Aoba, Aoba-ku, Sendai city, Miyagi, 980-8579 JAPAN

3 Dept. of Neurosurgery, School of Medicine, Fujita Health University, 1-98 Dengakugakubo, Kutsukake-cho, Toyoake city, Aichi, 470-1192 JAPAN

was used to observe surface and interior morphology of scaffolds.

2.2 Fabrication of magnetic porogens

Magnetic sugar particles (MSPs) as porogens were prepared by an emulsion technique. First, 60 g of D-fructose were melted at 120°C until a clear yellow liquid was obtained. Then 6 g of ferrite particles were added in the solution to append magnetism. The brown-colored liquefied fructose with ferrite particles was emulsified into 50 mL mineral oil with 1.3 mL Span 80 at 120°C under stirring. The suspension was cooled down rapidly using an ice-bath with effective stirring to solidify MSPs separately. Solidified MSPs were washed in hexane to remove mineral oil and surfactant completely. The diameter of MSPs was controlled between the different mesh sizes of two sieves in hexane. In this paper, we controlled the diameter of MSPs to 250-300 μm (MSPs 1) and 425-500 μm (MSPs 2).

2.3 Fabrication of porous PLCL sheet-like scaffolds

2.3.1 Scaffolds with widely dispersed pores

Figure 1 shows the fabrication process of PLCL sheet-like scaffolds with widely (several centimeters square) dispersed pores. First, PVA solution was spin-coated on a silicone wafer (1000 rpm, 30 seconds) and was dried in a hot oven (Fig. 1 (a)). MSPs fabricated in 2.2 were attracted to form an assembly by a neodymium magnet (magnetic flux density: 0.122 T) located under the wafer (Fig. 1 (b)). Then polymer solution (PLCL 10w% in chloroform) was dropped on MSPs and a vacuum was applied to fill the interspace between each particle. After the complete evaporation of chloroform and removal of the magnet, the composite with silicone wafer was soaked in water to dissolve the sugar and PVA. At this stage of dissolution, PVA contributed as a sacrificial layer[15] to the slow dissolution of MSPs. The dissolution of PVA and sugar was accelerated by an ultrasonic cleaner.

2.3.2 Scaffolds with polka-dot pattern of pores

Figure 2 shows the fabrication process of PLCL sheet-like scaffolds. A conventional patterning device comprising acryl(thickness: 5 mm) and steel wires (ϕ = 0.7 mm, 3 mm interval was utilized to generate polka-dot pattern of magnetic field on the surface[16]. A neodymium magnet (0.38 T) was placed under the patterning device. MSPs were attracted by a magnetic force to form polka-dot self-assembly. Molding of PLCL and dissolution of PVA and sugar were done in the same way as 2.3.1.

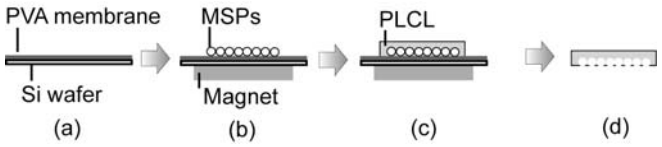

Fig. 1 Fabrication process of a sheet-like scaffold (a) PVA membrane is spin coated on a silicon wafer. (b) MSPs are self-assembled on the surface by magnetic attraction force. (c) Polymer solution is dropped on the self-assembled MSPs. (d) PVA as a sacrificial layer and MSPs are dissolved by water.

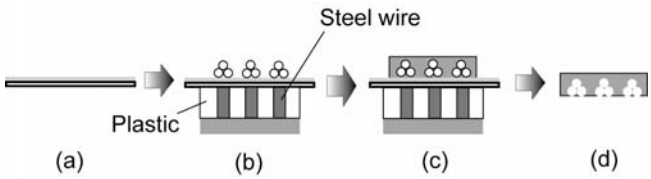

Fig. 2 Fabrication process of a sheet-like scaffold with polka-dot pattern of pores. Combination of plastic and steel wire was used to pattern MSPs.

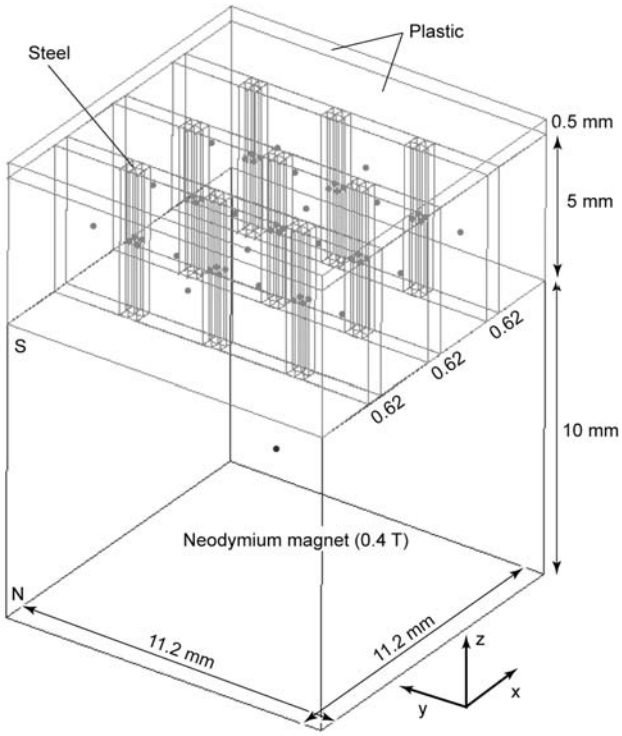

Fig. 3 Analytical model used for the calculation of magnetic flux density on the patterning device. Steel wires (ϕ = 0.7 mm) were replaced as square poles (0.62 x 0.62 x 5 mm) with the same cross-sectional area.

2.4 Analysis of magnetic flux density on the polka-dot patterning device

The magnetic flux density on the wafer surface was calculated using a magnetic simulation software (Super Moment, in Japanese [17]). The model for analysis is shown in Fig. 3. A block-type neodymium magnet (11.2 x 11.2 x 10 mm, 0.4 T), a patterning device (11.2 x 11.2 x 5 mm) that contains square poles of steel (0.62 x 0.62 x 5 mm, interval of 3 mm), and a plastic sheet was modeled to simplify the simulation. Steel wires were approximated as square poles with the same cross-sectional area.

2.5 Fabrication of porous PLCL tubular scaffolds

Figure 4 shows a fabrication process of a PLCL tubular scaffold. A PVA tube with arbitrary wall thickness (inner diameter > 1 mm) as a sacrificial model can be prepared as described previously (Fig. 4(a), [15]). Then a PLCL sheet-like scaffold fabricated in 2.3 was rolled around the tube with several millimeters' overlap (Fig. 4(b)(c)). After winding, the boundary of inner and outer sheet was welded by original polymer solution (PLCL 10w% in chloroform, Fig. 4(d)). After the dissolution of PVA sacrificial tube, we

obtained a PLCL cylindrical scaffold with controlled pore layouts (Fig. 4(e)).

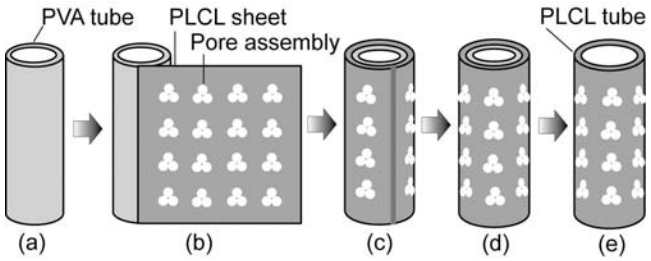

Fig. 4 Fabrication process of a tubular scaffold (a) PVA sacrificial tube was obtained by lost-wax method (b)(c) PLCL sheet with pores was rolled around the PVA tube. (d) The edge line of PLCL sheet was welded by original PLCL solution. (e) After the dissolution of PVA the tube, PLCL tubular construct with porous configuration was obtained.

2.6 Cell seeding and culture on scaffolds

Sheet-like PLCL scaffolds were developed in the same manner as described in 2.3.1. After oxidization and washing with 70% ethanol, the scaffolds were dried. During drying, HuMedia EG2, carbonic acid buffer and HEPES were added to neutralize the 0.5% type I collagen solution. The dried scaffolds were coated with neutral collagen under vacuum for 5 minutes. The collagen-coated scaffolds were kept at 37°C for 1 hour to initiate the formation of collagen gel, after which scaffolds were fixed onto the wells of a 6-well plate. Over 4 days, HUVECs were cultured in wells with scaffolds. (Cells were seeded on first and third day. Number of cells: 2.67 x 10^5 / well for each seeding, 5% CO_2)

2.7 Observation of HUVECs on scaffolds

An inverted optical microscope with a conventional fluorescent system was used to observe HUVECs on scaffolds. The scaffolds with seeded HUVECs were stained after being cultured for 4 days. After cell staining, the scaffolds were exposed to excitation light under the fluorescent microscopic system (blue excitation and green emission, (objective lens: 10x) SYTO 13 Green-fluorescent nucleic acid stains was used to observe cellular status on the scaffolds. The excitation and emission wavelengths of SYTO 13 dye in the presence of DNA were 488 nm and 509 nm, respectively.

III. RESULTS AND DISCUSSION

3.1 Fabrication of magnetic sugar microspheres

Owing to the activity of surfactant, liquefied D-fructose containing ferrite particles formed emulsion with mineral oil at 120°C. After the emulsification, MSPs were successfully solidified with little damage on their spherical shape. Figure 5 shows optical micrographs of MSPs with controlled diameter suspended in hexane. Ferrite micro/nano particles were successfully encapsulated in sugar microspheres. Table I shows the size distribution of MSPs 1 (Fig. 5(a)) and MSPs 2 (Fig. 5(b)) after sieving in hexane. In both cases, the average diameters of MSPs were relatively closer to the smaller mesh size. The successful manipulation of MSPs by external magnetic force supported the maintenance of magnetic function of ferrite particles after alternation of temperature from 120°C to 0°C.

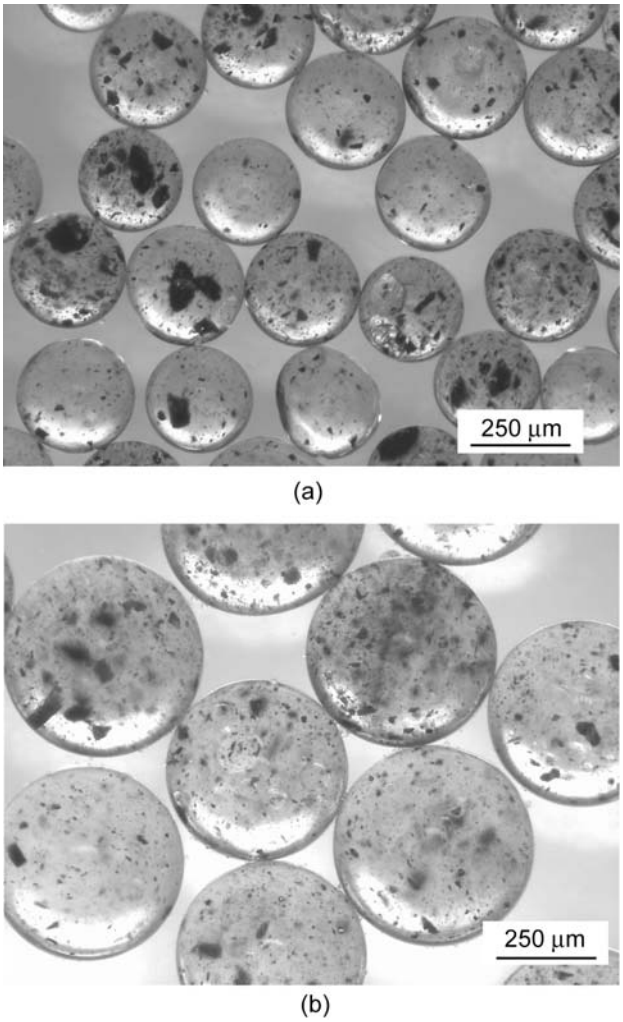

Fig. 5 Optical micrographs of emulsified, solidified and sieved MSPs in hexane. Ferrite particles (black sites) were successfully encapsulated in sugar microspheres. (a) MSPs sieved in the range of 250 - 300 µm (b) MSPs sieved in the range of 425-500 µm

Table I Size distribution of MSPs after sieving (average of 20 particles)

Sieving range	250 - 300 µm	425 - 500 µm
Average diameter	274 µm	459 µm
SD	18 µm	20 µm

3.2 Polka-dot pattern of self-assembled MSPs

Two-dimensional layout of MSPs on the PVA-coated silicon wafer determines the pore layout inside a scaffold at the stage of casting to polymer. We tried to assemble MSPs in a polka-dot pattern to generate patterned pores and to control the pore layout, porosity inside PLCL sheets. Figure 6 shows self-assembled MSPs 1 (Fig. 6(a)) and MSPs 2 (Fig. 6(b)) fabricated in 3.1. Owing to ferrite particles inside MSPs and 7 x 7 array of steel wires, MSPs formed polka-dot pattern on the surface of PVA-coated silicon wafer. Since the disk-type neodymium magnet hold the largest magnetic flux density around its circumference, larger number of MSPs were attracted to exterior wires.

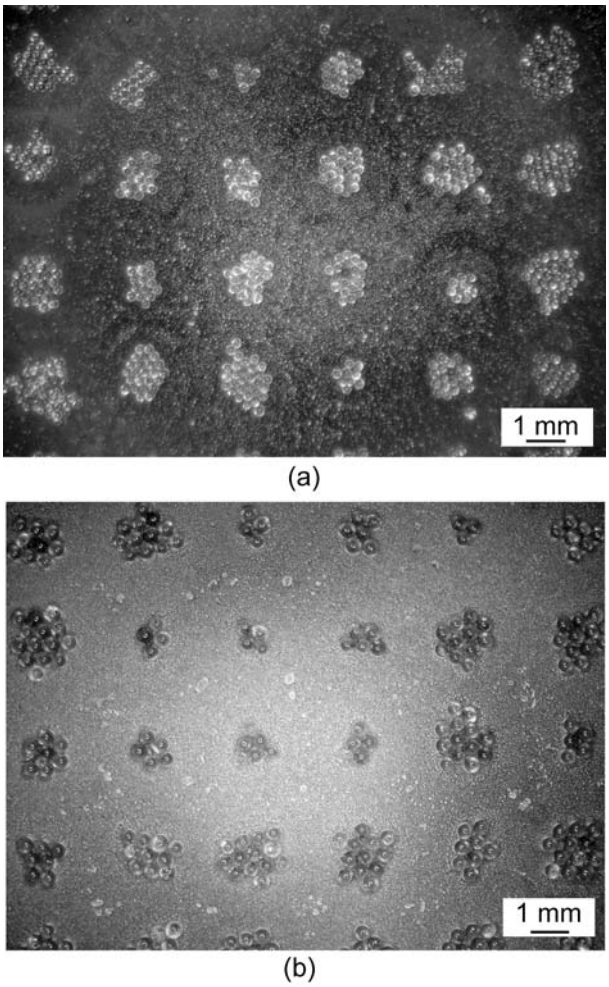

Fig. 6 Polka-dot pattern of self-assembled (a) MSPs 1 and (b) MSPs 2

3.3 Analysis of magnetic flux density on the patterning device

The magnetic flux density on the surface of PVA-coated silicon wafer was calculated using a simulation software (Fig. 7). 3D distribution of magnetic flux density to the z-direction (B_z) was acquired by measuring the value at the pitch of 0.2 mm to both x and y direction on the 11.2 mm square. After the calculation of magnetic moment analysis, polka-dot pattern of spiky magnetic field was confirmed on steel wires. The maximum value of B_z was 0.27 T when a neodymium magnet (0.4 T) was placed under the patterning device.

3.4 Fabrication and morphological evaluation of PLCL sheet-like scaffolds

3.4.1 Scaffolds with widely dispersed pores

MSPs shown in Fig. 5 were used to fabricate sheet-like scaffolds. After assembling MSPs on a PVA-coated silicon wafer and drying hexane, PLCL solution was dropped on the assembled MSPs as a casting template. Both MSPs 1 and MSPs 2 were successfully cast into PLCL as a biodegradable polymer. Figure 8(a) shows a sample surface configuration of PLCL sheet-like scaffold with widely dispersed pores. This sample was fabricated by casting from MSPs 2 (459 ± 20 μm).

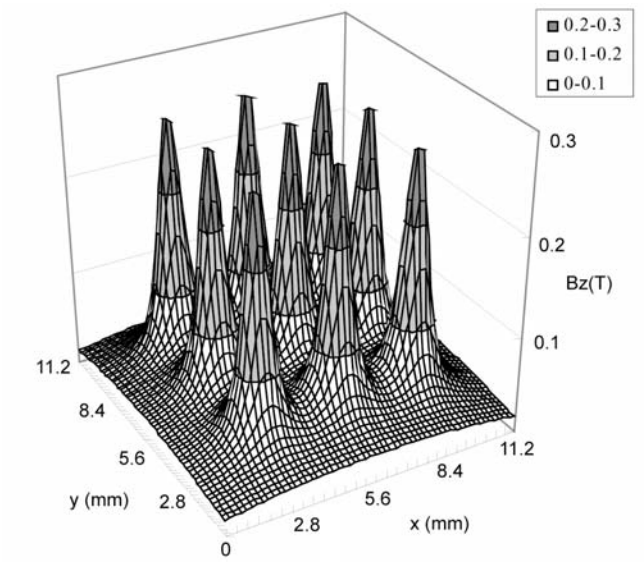

Fig. 7 Three-dimensional distribution of magnetic flux density

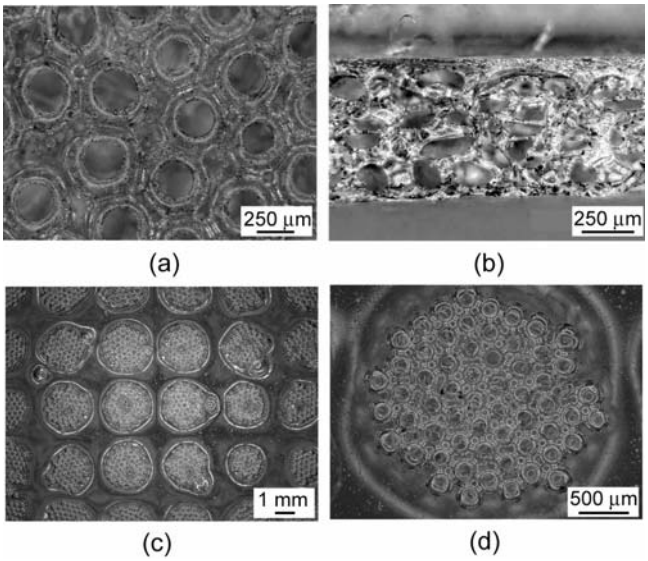

Fig. 8 Optical micrographs of PLCL sheet-like scaffolds. (a) Surface configuration of PLCL sheet with circular holes. (b) Cross-sectional image of (a). (c) Surface configuration of PLCL sheet with polka-dot array of pore assembly. (d) Magnified image of a dot in (c).

Table II Diameter of holes after polymer casting (average of 20 holes)

MSPs used for casting	MSPs 1	MSPs 2
Average diameter	161 μm	220 μm
SD	13 μm	30 μm

Figure 8(b) shows a cross-sectional image of the same scaffold.In this image, 2D images at different focal point were synthesized to obtain 3D information. Well-connected pores owing to magnetically-guided self-assembly were confirmed. The diameter of holes on the surface was evaluated in Table II. These holes were generated by the contact between MSPs and PVA surface. Although sugar particles were originally spherical, they deform at the contact point by heat and humidity in atmosphere. The diameters of these holes were reasonably smaller than those of original MSPs.

3.4.2 Scaffolds with polka-dot pattern of pores

Polka-dot pattern of MSPs shown in Fig. 6 was cast into PLCL sheet. Figure 8(c) shows the surface of PLCL sheet with polka-dot pattern of pore assembly. A magnified image of single pore assembly is shown in Fig. 8(d). Spherical shape of MSPs was successfully patterned inside PLCL with little damage. Especially in this case, PVA thin film as a sacrificial layer contributed to the mild detachment of PLCL sheet from the silicon wafer, thereby causing little damage to pore shape.

Owing to the magnetically-guided self-assembly of MSPs, we can control the pore layout inside 2D polymer sheet by changing following parameters; (i) interval length between steel wires (ii) diameter of steel wires (iii) diameter of MSPs (iv) amount of MSPs. The smallest limitation of MSPs that can be cast into PLCL is 50 μm. However, we believe that the size is appropriate when we consider to introduce cells (c.a. 10 μm) inside pores.

3.5 Fabrication of PLCL tubular scaffolds

Sheet-like scaffolds fabricated in 3.4 were used to fabricate tubular scaffolds. Scaffolds were rolled around PVA sacrificial tubes and the edge line between inner and outer layer was welded by original PLCL solution. After drying and dissolution of the PVA sacrificial tube, tubular scaffolds were successfully obtained as shown in Fig. 9.

We chose PLCL in terms of bioactivity[18] and mechanoactivity[19] for future application in vascular tissue engineering. Initially, we tried to assemble MSPs around the cylindrical surface by using a cylindrical bar magnet. However, theoretically it is almost impossible to generate a uniform magnetic field all over the surface, especially if its axial length becomes longer than 1 cm. When we consider the application in vascular tissue engineering, this method of winding a sheet with use of MSPs will be the better way to control the pore layout and porosity inside a small-diameter vascular graft.

So far, straight cylindrical vascular grafts have been fabricated by electrospinning[5,18,19] or excimer laser ablation[20]. In the case of electrospinning, it is very difficult to control pore layout to the axial direction. In the case of excimer laser ablation, they spent 8 hours to fabricate a vascular graft with 2 cm length. Compared with these methods, our method can create patterned porous configuration in 2D plane by use of patterned magnetic field and 2D sheets can be easily rolled to tubes in a short time regardless of tube size (total fabrication time < 4 hours). The maximum axial length and minimum inner diameter available by this method are 4 cm and 1 mm, respectively.

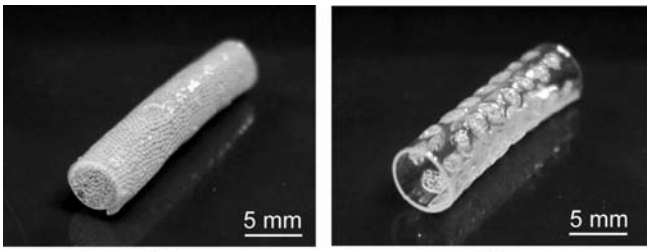

Fig. 9 (a) PLCL tubular scaffold with porous structure all over the inner surface (b) PLCL tubular scaffold with polka-dot pattern of pores

3.6 Cultured HUVECs on a sheet-like scaffold

Figure 10 shows a fluorescent micrograph of nucleic acids of HUVECs on a scaffold. White sites indicate nucleic acids of HUVECs. Because the sheet-like scaffold has 3D porous structure, some cells were observed out of the focal plane. Sparsely scattered black sites indicate residual ferrite particles. We believe these ferrite particles have little damage on cell growth and morphology because cells containing ferrite particles have been cultured by some groups [13,16,17]. According to the cohesive and viable HUVECs after 4-day in vitro cell culture, our fabrication method and used materials are at least safe for cell culture.

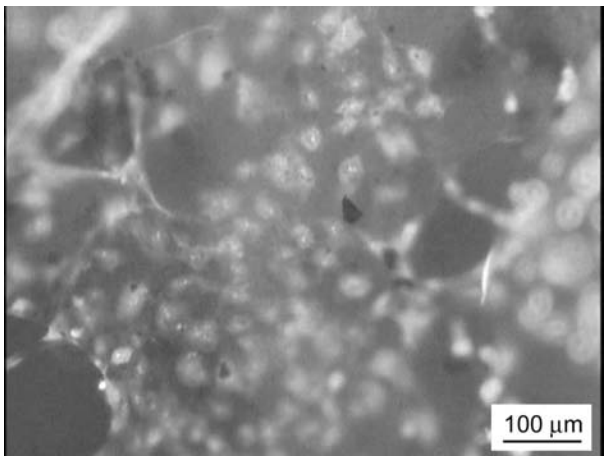

Fig. 10 A fluorescent micrograph of HUVECs attached on a sheet-like scaffold. White sites indicate the location of viable HUVECs.

IV. CONCLUSION

The functionalization of porogen will be very useful to expand and break through the fabrication range of biodegradable scaffolds and biological substrates. In this paper, we proposed a novel method to develop porous biodegradable scaffolds by use of MSPs as the world's first magnetic porogens. MSPs were successfully manipulated, assembled and patterned to form a casting template by external magnetic force. The diameter of MSPs was highly tunable by using sieves in hexane. Those diameter-controlled particles were utilized to fabricate flat and tubular PLCL constructs. As future works, we are currently exploring applications of tubular scaffolds as small-diameter vascular grafts. Additionally, the development of biomimetic vascular substitute will be very effective to evaluate robotic manipulation of catheters for endovascular surgery.

V. ACKNOWLEDGMENT

The authors thank Toda Kogyo for the provision of ferrite particles and Mr. Hideo Matsuura for the fabrication of experimental jigs. The authors also thank Prof. Hiroyuki Honda and Mr. Kosuke Ino for allowing us to use the cell

culture environments. This research work was funded by Grant-in-Aid for the 21st Century COE "Micro- and Nano-Mechatronics for Information-Based Society". This work was also funded by Grant-in-Aid for Scientific Research on Priority Areas, "System cell engineering by multi-scale manipulation".

REFERENCES

[1] R. Langer, J.P. Vacanti, "Tissue engineering", *Science* 260, 920-926 (1993)

[2] L.G. Griffith, G. Naughton, "Tissue engineering – Current challenges and expanding opportunities", *Science* 295, 1009-1014 (2002)

[3] A. Khademhosseini, R. Langer, J. Borenstein, J.P. Vacanti, "Microscale technologies for tissue engineering and biology", *Proc. Natl. Acad. Sci. U.S.A.* 103, 2480-2487 (2006)

[4] J. Gao, P.M. Crapo, Y.D. Wang, "Macroporous elastomeric scaffolds with extensive micropores for soft tissue engineering", *Tissue Eng.* 12, 917-925 (2006)

[5] S. Kidoaki, I.K. Kwon, T. Matsuda, "Mesoscopic spatial designs of nano- and microfiber meshes for tissue engineering matrix and scaffold based on newly devised multilayering and mixing electrospinning techniques", *Biomaterials* 26, 37-46 (2005)

[6] A.G. Mikos, G. Sarakinos, S.M. Leite, J.P. Vacanti, R. Langer, "Laminated three-dimensional biodegradable foams for use in tissue engineering", *Biomaterials* 14, 323-330 (1993)

[7] C.J. Bettinger, E.J. Weinberg, K.M. Kulig, J.P. Vacanti, Y.D. Wang, J.T. Borenstein, R. Langer, "Three-dimensional microfluidic tissue-engineering scaffolds using a flexible biodegradable polymer", *Adv. Mater*. 18, 165-169 (2006)

[8] V. Mironov, T. Boland, T. Trusk, G. Forgacs, R.R. Markwald, "Organ printing: computer-aided jet-based 3D tissue engineering", *Trends Biotechnol.* 21, 157-161 (2003)

[9] Y.S. Nam, T.G. Park, "Biodegradable polymeric microcellular foams by modified thermally induced phase separation method", *Biomaterials* 20, 1783-1790 (1999)

[10] W.L. Murphy, R.G. Dennis, J.L. Kileny, D.J. Mooney, "Salt fusion: An approach to improve pore connectivity with tissue engineering scaffolds", *Tissue Eng.* 8, 43-52 (2002)

[11] G.B. Wei, P.X. Ma, "Macroporous and nanofibrous polymer scaffolds and polymer/bone-like apatite composite scaffolds generated by sugar spheres", *J. Biomed. Mater. Res. A*, 78A, 306-315

[12] E. Alsberg, E. Feinstein, M.P. Joy, M. Prentiss, D.E. Ingber, "Magnetically-Guided Self-Assembly of Fibrin Matrices with Ordered Nano-Scale Structure for Tissue Engineering", *Tissue Eng.* 12, 3247-3255 (2006)

[13] A. Ito, K. Ino, M. Hayashida, T. Kobayashi, H. Matsunuma, H. Kagami, M. Ueda, H. Honda, "Novel methodology for fabrication of tissue-engineered tubular constructs using magnetite nanoparticles and magnetic force", *Tissue Eng.* 11, 1553-1561 (2005)

[14] S.J. Bryant, J.L. Cuy, K.D. Hauch, B.D. Ratner, "Photo-patterning of porous hydrogels for tissue engineering", *Biomaterials* 28, 2978-2986 (2007)

[15] T. Uchida, S. Ikeda, H. Oura, M. Tada, T. Nakano, T. Fukuda, T. Matsuda, M. Negoro, F. Arai, "Development of biodegradable scaffolds based on patient-specific arterial configuration", *J. Biotechnol*. 133, 213-218 (2008)

[16] K. Ino, A. Ito, H. Honda, "Cell patterning using magnetite nanoparticles and magnetic force", *Biotechnol. Bioeng.* 97, 1309-1317 (2007)

[17] K. Ino, M. Okochi, N. Konishi, M. Nakatochi, R. Imai, M. Shikida, A. Ito, H. Honda, "Cell culture arrays using magnetic force-based cell patterning for dynamic single cell analysis", *Lab Chip* 8, 134-142 (2008)

[18] H. Inoguchi, T. Tanaka, Y. Maehara, T. Matsuda, "The effect of gradually graded shear stress on the morphological integrity of a huvec-seeded compliant small-diameter vascular graft", *Biomaterials* 28, 486-495 (2007)

[19] I.K. Kwon, S. Kidoaki, T. Matsuda, "Electrospun nano- to microfiber fabrics made of biodegradable copolyesters: structural characteristics, mechanical properties and cell adhesion potential", *Biomaterials* 26, 3929-3939 (2005)

[20] H. Sonoda, K. Takamizawa, Y. Nakayama, H. Yasui, T. Matsuda, "Coaxial double-tubular compliant arterial graft prosthesis: time-dependent morphogenesis and compliance changes after implantation", *J. Biomed. Mater. Res. A* 65A, 170-181 (2003)